

pubs.acs.org/jmc Article

Inhibition of the Ubiquitin Transfer Cascade by a Peptidomimetic Foldamer Mimicking the E2 N-Terminal Helix

Li Zhou, In Ho Jeong, Songyi Xue, Menglin Xue, Lei Wang, Sihao Li, Ruochuan Liu, Geon Ho Jeong, Xiaoyu Wang, Jianfeng Cai,* Jun Yin,* and Bo Huang*

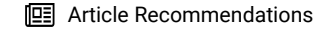


Cite This: J. Med. Chem. 2023, 66, 491-502



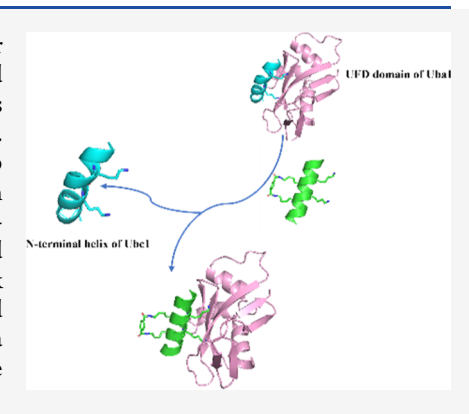
ACCESS I

Metrics & More



Supporting Information

ABSTRACT: The enzymatic cascades for ubiquitin transfer regulate key cellular processes and are the intense focus of drug development for treating cancer and neurodegenerative diseases. E1 is at the apex of the UB transfer cascade, and molecules inhibiting E1 have shown promising activities against cancer cell proliferation. Compared to small molecules, peptidomimetics have emerged as powerful tools to disrupt the protein-protein interactions (PPI) with less drug resistance and high stability in the cell. Herein, we harnessed the D-sulfono-γ-AA peptide to mimic the Nterminal helix of E2 and thereby inhibit E1-E2 interaction. Two stapled peptidomimetics, M1-S1 and M1-S2, were identified as effective inhibitors to block UB transfer from E1 to E2, as shown by in vitro and cellular assays. Our work suggested that PPIs with the N-terminal helix of E2 at the E1-E2 and E2-E3 interfaces could be a promising target for designing inhibitors against protein ubiquitination pathways in the cell.



■ INTRODUCTION

Ubiquitin (UB) is a 76-residue protein, and it rides on the UB transfer cascades constituted by the E1, E2, and E3 enzymes for its delivery to a broad spectrum of cellular targets to control their stability, localization, movement, and biological activities in the cell. 1,2 The ubiquitin-proteasome system (UPS), consisting of the UB transferring enzymes for conjugating UB to the cellular targets, the deubiquitinating enzymes for removing the UB modification, and the proteasome for proteolytic processing of ubiquitinated proteins, regulates key processes in the cell, including cell cycle, DNA repair, protein quality control, autophagy, and programed cell death. 3-6 Various components of the UPS have emerged as promising targets of the drug discovery pipeline, and the development of bortezomib, a proteasome inhibitor for the treatment of multiple myeloma, substantiates the premise of targeting UPS for the treatment of challenging diseases such as cancer and neurodegeneration.^{7–12} Still, the extensive protein-protein interactions (PPIs) that mediate UB transfer through the E1-E2-E3 cascade create a significant hurdle for designing small molecules to block UB transfer through specific cascades to achieve the desired therapeutic effects. 13-15 Here, we demonstrated that the E1-E2 interface relying on the binding of an N-terminal helix of E2 with the E1 enzyme could be effectively targeted by synthetic peptidic foldamers composed of the D-sulfono- γ -amino acids (γ -AA) building blocks. The designed sulfono- γ -AA peptides have a strong tendency to adopt an α -helical fold and can compete with E2 for occupying the binging site on E1. This enables the γ -AA

peptide to block UB transfer through the E1-E2-E3 enzymatic cascade and inhibit substrate ubiquitination in the cell.

The human genome encodes two homologous E1 enzymes known as Uba1 and Uba6 to activate the C-terminal carboxylate of UB accompanied by ATP hydrolysis for the formation of E1~UB thioester conjugates between the catalytic Cys residue of E1 and the C-terminal Gly residue of UB. 16,17 Subsequently, UB is transferred by E1 to a catalytic Cys residue of E2 that carries UB to the E3 enzymes for further transfer of UB to the target proteins recruited by the E3. The N-terminal helix of E2 is a major element of recognition at both the E1-E2 and E2-E3 interfaces. 18-20 On the E1 side, the N-terminal helix of E2 would bind to the ubiquitin fold domain (UFD) of Uba1 and Uba6 through a series of salt bridges (Figure 1a),²¹ and on the E3 side, the N-terminal helix of E2 would dock to E3s of varies classes such as HECT, Ring, and U-box at their unique binding sites.^{22–25} The essential roles of the N-terminal helix of E2 in engaging E1 and E3 have been manifested in the recent engineering of orthogonal ubiquitin transfer (OUT) cascades to generate exclusive interactions within the xE1-xE2 and xE2xE3 pairs to enable the transfer of an engineered xUB to cellular targets of a specific E3.26,27 We rationalize that a synthetic

Received: September 4, 2022 Published: December 26, 2022





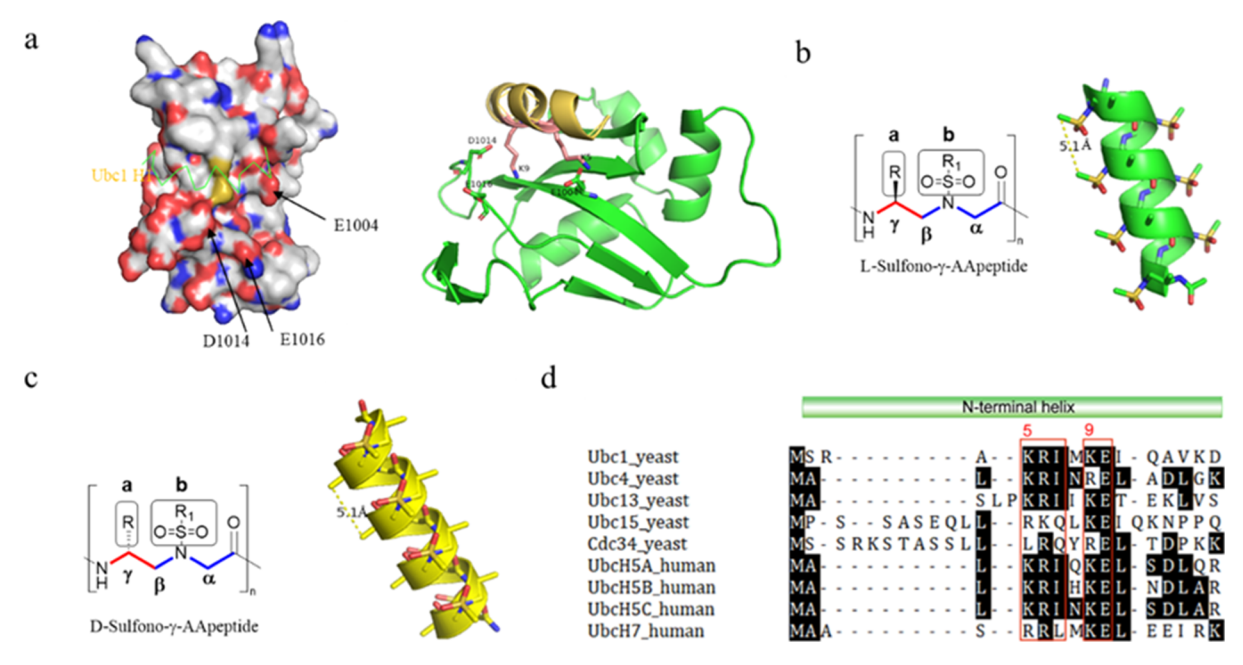


Figure 1. Structural information for designing peptide foldamers mimicking the N-terminal helix of E2 enzymes. (a) Structures of the UFD domain of Uba1 (E1) binding to the N-terminal helix of Ubc1 (E2). The model was created by using Pymol, starting from a reported crystal structure of the Uba1—UB complex (PBD ID: 3CMM) and Ubc1 (PBD ID: 1TTE). Electrostatic surface represents the negatively charged surface of the UFD domain of Uba1 for interacting with the N-terminal helix of the E2 enzyme Ubc1 (Left) and residues involved in the interaction between the UFD of Uba1 and the N-terminal helix of Ubc1 (Right). (b) Chemical structures of the homogeneous L-sulfono-γ-AA peptide and the crystal structure of the L-sulfono-γ-AA peptide. "a" and "b" denote the chiral side chain and sulfono side chain, respectively. (c) Chemical structures of the homogeneous D-sulfono-γ-AA peptide and the three-dimensional structure of the D-sulfono-γ-AA peptide. (d) Multiple sequence alignment of several E2 enzymes. Residues that are conserved at the E1–E2 interface are highlighted with a red frame. The alignment only includes residues in the N-terminal helix of E2 and adjacent residues.

peptide mimic of the E2 N-terminal helix can potentially compete with E2 for binding to the upstream E1 and downstream E3 of the UB transfer cascade, and such modality could be a competent inhibitor counteracting the substantial PPIs at the native E1–E2 and E2–E3 interfaces.

Our design harnessed the strong α -helix-like forming potential of the sulfono-γ-AA peptide that was introduced as a class of unnatural peptidomimetic foldamers that offers unique advantages such as robust helical folding propensity, stability, diversity, and bioavailability. 28-32 The crystal structures of homogeneous L-sulfono-γ-AA peptides reveal that they adopt 4_{14} left-handed helices with a helical pitch of 5.1 Å³³ (Figure 1b), highly analogous to that of the α -helix (5.4 Å). To this end, we have successfully employed them as potential therapeutic agents to mimic a plethora of essential protein domains and modulate medicinally relevant PPIs such as VEGF, 34 BLC9, 35 p53, 36-38 and GLP-1.³⁹ However, the opposite helical handedness of Lsulfono- γ -AA peptides, in contrast to that of the α -helix, may potentially complicate the design of PPI inhibitors, particularly when residues on the multiple faces of the α -helix are involved at the protein-protein interfaces. Therefore, we recently replaced L-sulfono-γ-AA building blocks with D-sulfono-γ-AA building blocks in the homogeneous D-sulfono- γ -AA peptides, leading to the formation of right-handed helices from their mirror-imaged left-handed helices (Figure 1c).³⁷ Since the helicity of Dsulfono- γ -AA peptides is the same as that of the α -helix, the design of the γ -AA peptides mimicking the α -helix would be much simplified based on their similar distribution of side chains on the helical wheel (Figure S1).

RESULTS

Rational Design of the D-Sulfono-γ-AA Peptide to Mimic the N-Terminal Helix of E2. The E1-E2 interface of the UB transfer cascade was first revealed by a modeled structural complex between the two yeast enzymes Uba1 and Ubc1 that shows the N-terminal helix of Ubc1 engaging the UFD domain of Uba1 through salt bridge interactions between positively charged E2 helical residues K5 and K9 and negatively charged E1 UFD residues E1004, D1014, and E1016.²¹ The importance of K5 and K9 in bridging Ubc1 binding with Uba1 was confirmed by phage selection of a Ubc1 library with randomized sequence in the N-terminal helix for its recognition by a Uba1 mutant with charge-reversed mutations E1004K, D1014K, and E1016K in the UFD region.²⁷ The selection based on UB transfer from the Uba1 mutant to the Ubc1 library displayed on the phage surface enriched sequences, with D and E replacing K5 and K9 in the N-terminal helical region so that the mutant Ubc1 could reestablish the interaction with the chargereversed Uba1 mutant. Such a result corroborates with the structural model of the Uba1-Ubc1 complex and suggests that the interaction of K5 and K9 of the N-terminal helix of E2 represented by Ubc1 could be a promising target to design γ -AA peptide inhibitors to block E1-E2 interactions. Furthermore, the recent elucidation of the crystal structures of yeast Uba1 in complex with Ubc4, Ubc15, and Cdc34 all suggest that E2 Nterminal helical residues aligned with K5 and K9 in Ubc1 would play critical roles for interacting with the UFD domain of Uba1 (Figure 1d).^{40–43}

The N-terminal helix of yeast E2 Ubc1 is highly homologous to the human E2 UbcH5B with K4 and K8 occupying the positions of K5 and K9 in Ubc1 (Figure 1d). The yeast E1 Uba1

Table 1. Structures of the D-Sulfono-γ-AA Peptide and Ubc1 Alpha-1-Helix^a

	Ubc1 alpha-1 helix		Linear D-sulfono-γ-AA peptide
NI		M1	NH2
	H & CH & I H & H & CH & CH & CH & CH & C	M2	NH ₂
Stapled D-sulfono-γ-AA peptide			
M1-S1	NH2	M2-S1	
M1-S2		M2-S2	
M1-S3		M2-S3	HO STATE OF THE ST

^aResidues involved in the interaction with the UFD domain of E1 are shown in red.

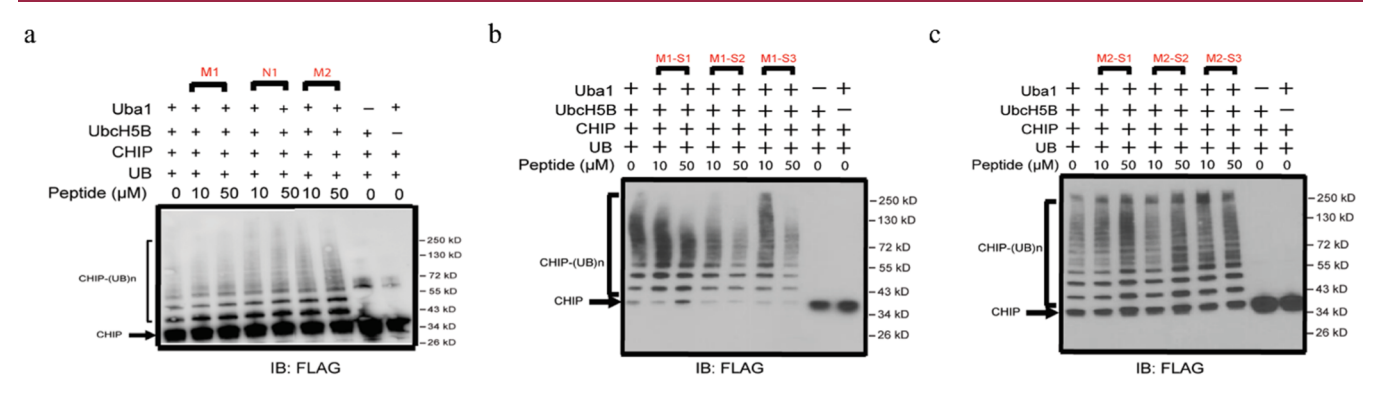


Figure 2. Effect of linear sulfono γ -AA peptides and stapled sulfono γ -AA peptides on the self-ubiquitination of CHIP. (a) Assaying the effects of linear peptides on ubiquitin transfer based on the self-ubiquitination of CHIP. CHIP self-ubiquitination was measured by western blotting probed with an anti-Flag antibody that binds to the Flag—tagged CHIP. M1 and M2 are γ -AA peptides mimicking the sequence of the N-terminal helix of Ubc1, and N1 is the native peptide with the same sequence as the N-terminal helix of Ubc1. None of these peptides showed an inhibitory effect on the CHIP polyubiquitination. CHIP-(UB)_m polyubiquitinated CHIP. (b,c), Assaying the effects of stapled peptidomimetics on the UB transfer based on the polyubiquitination of CHIP. Ubiquitination of CHIP was measured by western blotting probed with an anti-Flag antibody that binds to the Flagtagged CHIP. All stapled peptidomimetics derived from M1 had an inhibitory effect on the polyubiquitination of CHIP, while other peptidomimetics derived from M2 did not inhibit the polyubiquitination of CHIP, and some may enhance CHIP ubiquitination.

is also homologous to human Uba1. We thus selected the N-terminal helix of Ubc1 as our initial template for designing the γ -AA peptides. Since D-sulfono- γ -AA peptides form a right-handed helix as natural α -peptides (Figures 1c and S1), the chiral side chains 1a, 3a, 5a, and 7a should align on the same side of the helical scaffold of the folded peptide. We thus have Lys side chains at 3a and 5a, so they would be in the similar positions as that of K5 and K9 in Ubc1. We initially designed two γ -AA

peptide sequences M1 and M2 to mimic the N-terminal helix of Ubc1. Since the stapled helical peptides have a more α -helical folding propensity and exhibit improved membrane permeability and proteolytic stability, ⁴⁴ we also designed M1 and M2 derivatives with staples crosslinking various AA peptide residues that are anchored to the opposite side of the binding interface with the UFD domain of Uba1 (Table 1). An overlay of peptide M1 or M1–S1 (Figure S2) with the alpha-1 helix of Ubc1

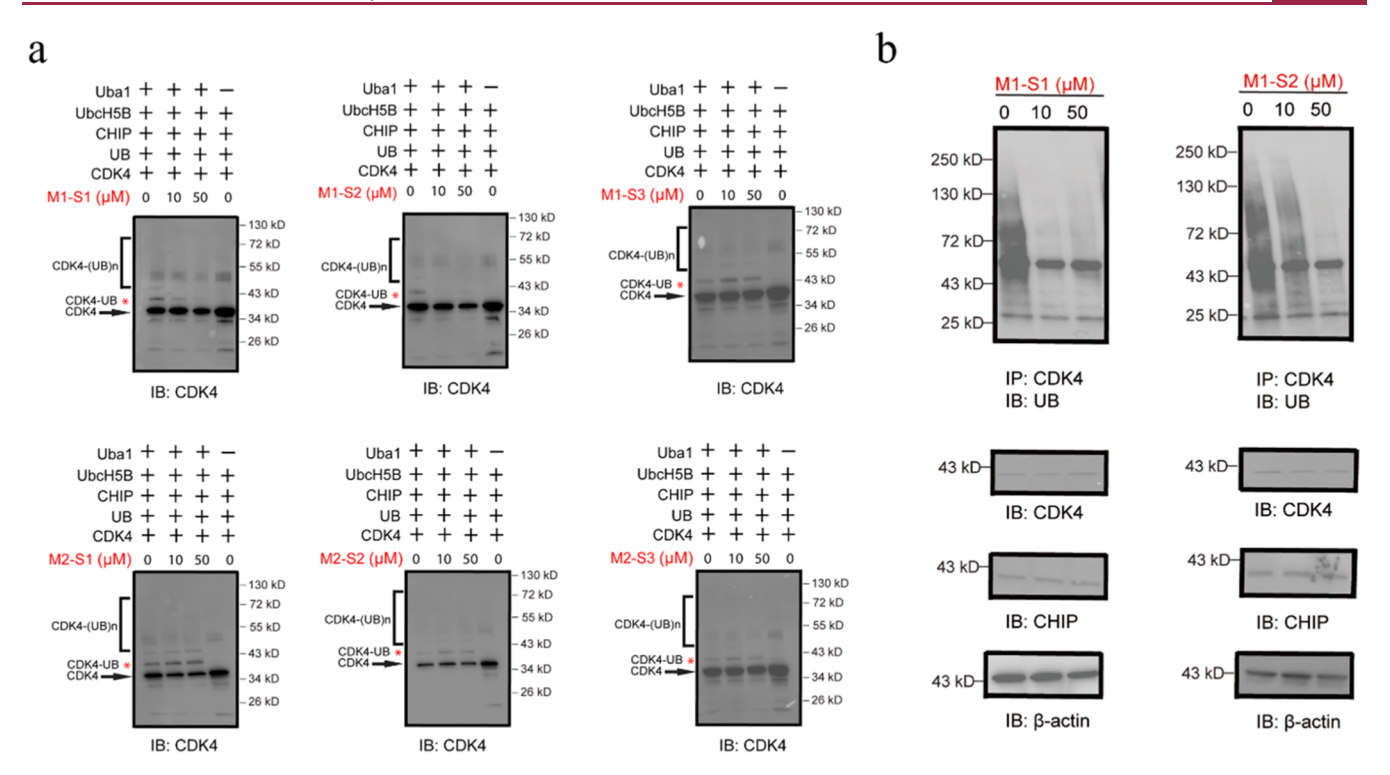


Figure 3. Effect of stapled sulfono γ -AA peptides on the monoubiquitination of CHIP substrate CDK4 *in vitro* and in the cell. (a) Measuring the effects of stapled peptides on CDK4 ubiquitination *in vitro*. The ubiquitination reaction contains 10 or 50 μM peptides incubating with the Uba1-UbcHSB-CHIP cascade and CDK4 as the CHIP substrate. M1–S1 and M1–S2 showed significant inhibition of the CDK4 ubiquitination in the reconstituted reaction. CDK4-UB, monoubiquitinated CDK4. CDK4-(UB)_m polyubiquitinated CDK4. (b) Measuring the effects of M1–S1 and M1–S2 on CDK4 ubiquitination in HEK293 cells. M1–S1 and M2–S2 inhibited the ubiquitination of CHIP substrate CDK4 in HEK293T cells. Each peptide of 0, 10, and 50 μM concentration was incubated with HEK293T cells for 14 h, and cells were treated with the proteasome inhibitor MD132 for another 12 h. The cells were harvested, and CDK4 was immunoprecipitated with an anti-CDK4 antibody from the cell lysate. The ubiquitination levels of CDK4 were measured by western blots probed with an anti-UB antibody. The images for the immunoblotting of CDK4 and CHIP indicated the equal input of total proteins. β-Actin was used an internal reference to confirm the equal loading of the cell lysate in each well.

suggested a good overlap between the designed side chains on the γ -AA peptide and the native sides chains of the E2 N-terminal helix, especially, side chains 3a and 5a of the γ -AA peptide are well positioned to replace residues Lys5 and Lsy9 of the E2 helix to bind to E1.

Activities of the Designed γ -AA Peptides to Inhibit the UB Transfer Cascade in the Reconstituted Ubiquitination Reaction. We assayed the potential inhibitory activities of the designed γ -AA peptides in inhibiting the self-ubiquitination of U-box E3 CHIP through the Uba1-UbcH5B-CHIP cascade. We found that the liner peptides M1 and M2 did not inhibit CHIP self-ubiquitination at either 10 or 50 μ M of the peptide concentration (Figure 2a). However, the stapled peptides derived from the M1 peptide can significantly inhibit CHIP self-ubiquitination at a concentration of 50 μ M based on the less formation of polyubiquitinated species in the high molecular range of the western blot (Figure 2b). CHIP itself was still ubiquitinated in the reactions with the peptide inhibitors, so the unmodified CHIP was consumed. However, CHIP polyubiquitination was significantly suppressed by the peptide inhibitors, suggesting the inhibitory effects of the peptides on UB transfer from Uba1 and UbcH5B to CHIP. In contrast, the stapled version of M2 peptides did not show significant inhibition of CHIP polyubiquitination at the same peptide concentration (Figure 2c). We thus further characterize the activity of the stapled sulfono-γ-AA peptides to inhibit CHIP-mediated ubiquitination of cyclin-dependent kinase 4 (CDK4) in vitro and in the cell. CDK4 was previously identified as a CHIP

substrate with the OUT cascade of the E3 constructed by engineering specific interactions between the N-terminal helix of UbcH5B with the UFD domain of Uba1 and the U-box domain of CHIP. 45

Activities of the Designed Stapled Peptides in Inhibiting CHIP-Mediated Ubiquitination of CDK4 In *Vitro* and in the Cell. To determine whether stapled mimetics could regulate the ubiquitination of CDK4, we incubated all stapled peptides at a concentration of 10 or 50 μ M in a reconstituted reaction with Uba1, UbcH5B, CHIP, CDK4, and HA-tagged UB. As shown in Figure 3a, M1-S1 and M1-S2 are highly effective at inhibiting ubiquitin transfer to substrate protein CDK4 by blocking its monoubiquitination catalyzed by CHIP, whereas other peptides showed no inhibitory activity of CDK4 monoubiquitination compared to the control reaction without adding the peptides. We then assayed if the two stapled peptides would affect the ubiquitination of CDK4 in the cell. We incubated HEK293T cells with 10 or 50 μ M M1-S1 or M1-S2 for 14 h, respectively. Then, we added MG132, a proteasome inhibitor, to suppress the degradation of ubiquitinated proteins in the cell and collected the total cell lysate to analyze the ubiquitination levels of substrate proteins by western blotting probed with an anti-UB antibody. Consistently, both stapled peptides could significantly inhibit the ubiquitination of CDK4 in the cell compared to the control reaction with no peptides added (Figure 3b). These results suggest that the designed peptide can function as an inhibitor of the UB transfer cascade to block the ubiquitination of E3 substrates.

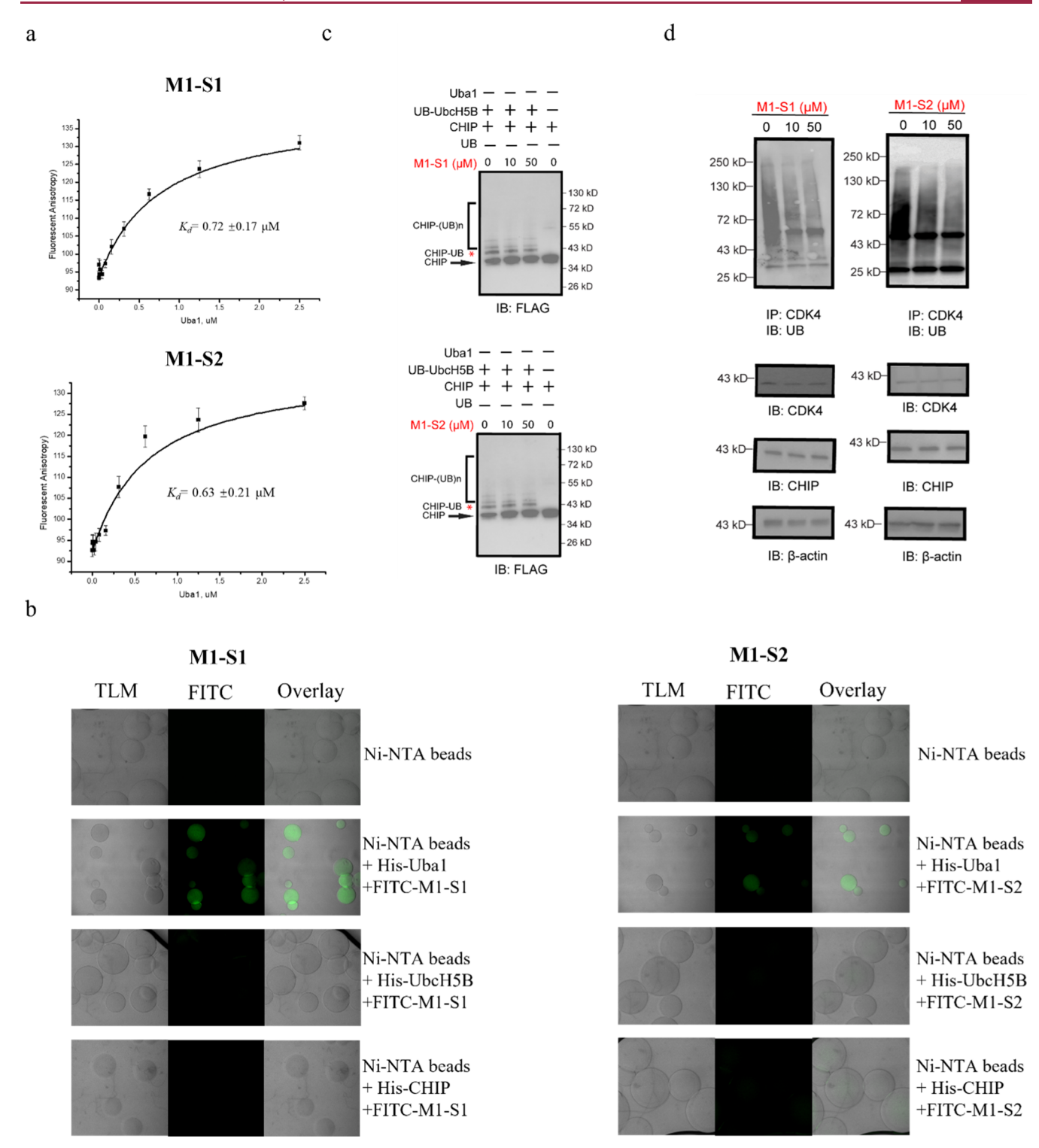


Figure 4. Specific binding of M1–S1 and M1–S2 with Uba1. (a) C-terminally FITCylated M1–S1 and M1–S2 bound to Uba1 with $K_{\rm d}$ values of 0.72 \pm 0.17 and 0.63 \pm 0.21 μ M, respectively. Binding affinity was assessed by FP assays. Error bars = standard deviation from three independent experiments. (b) Fluorescent bead binding assay showed that FITCylated M1–S1 and M1–S2 exhibited no non-specific binding to Ni-NTA beads (first row), selective binding to His-tagged Uba1-coated beads (second row), and no non-specific binding to beads coated with His-tagged UbcH5B or His-tagged CHIP (third and fourth row). TLM, transmission light microscopy. (c) No inhibitory activity of the M1–S1 and M1–S2 peptides was found when pre-ubiquitinated E2 was used to support CHIP self-ubiquitination. The ubiquitination reaction contains 0, 10, or 50 μ M concentration of peptides incubating with UB-UbaH5B and CHIP. CHIP-UB, monoubiquitinated CHIP. CHIP-(UB), polyubiquitinated CHIP. (d) Measuring the effects of M1–S1 and M1–S2 on CDK4 ubiquitination in HEK293 cells with overexpressed CHIP. M1–S1 and M1–S2 inhibited the ubiquitination of CHIP substrate CDK4 despite the enhanced levels of CHIP.

Binding Affinities of the Stapled Peptides with Uba1. We conducted a fluorescence polarization (FP) assay to measure

the binding affinity of stapled peptides with Uba1 (E1), UbcH5B (E2), and CHIP (E3), respectively. We also include

linear peptide M1 as a control. As shown in Figures 4a and S3a, M1–S1 and M1–S2 have $K_{\rm d}$ values of 0.72 and 0.63 μ M, respectively, for binding to Uba1, while no binding of the peptides with UbcH5B and CHIP was detected. Besides, in a fluorescence microscopy-based qualitative binding assay, fluorescein isothiocyanate (FITC)-labeled peptides were incubated with Ni-NTA beads preloaded with His-tagged Uba1, His-tagged Ubch5B, or His-tagged CHIP, respectively, and then, the beads were isolated by centrifugation and visualized. Consistently, Uba1-coated beads showed robust green fluorescence, suggesting a strong binding with the FITC-labeled peptides, whereas no binding was found between the peptide and beads immobilized with UbcH5B or CHIP or between linear peptide M1 and Uba1-coated beads (Figures 4b and S3b).

To further confirm that the peptides targeted E1 specifically, we tested in vitro UB transfer to CHIP from UbcH5B preloaded with UB while free UB or Uba1 were excluded from the reaction. As expected, no inhibition on self-ubiquitination of CHIP was observed in the presence of various concentration of D-sulfonoγ-AA peptides since the E2 enzyme UbcH5B is preloaded with UB and UB is no longer dependent on Uba1 for transferring to CHIP (Figure 4c). Moreover, while assaying CDK4 ubiquitination in HEK293 cells, we found a strong inhibitory effect of the M1-S1 and M1-S2 peptides on the ubiquitination of CDK4, despite the overexpression of CHIP in the cell. This suggests that the UB transfer cascade was blocked at the E1-E2 interface before UB could reach CHIP and its substrate proteins (Figure 4d). All these results demonstrated that stapled peptides M1-S1 and M1-S2 were effective in inhibiting the protein ubiquitination cascade by binding with Uba1, the E1 enzyme, and blocking UB transfer from E1 to E2.

Inhibition of UB Transfer to Different Types of E2 Enzymes. To assess the generalized inhibitory capacity of our peptides, we performed UB transfer assays *in vitro* with different types of E2 enzymes, including UbcH5B and UbcH7. As shown in Figure 5, M1−S1 and M1−S2 could significantly inhibit the formation of E2∼UB conjugates at 50 μM concentration of the peptide. This proves that the stapled peptides would dock to E1 and disrupt E1−E2 interaction.

Circular Dichroism Measurements. To assess the conformational advantage of our sulfono-γ-AA peptide-based peptidomimetics, circular dichroism (CD) studies were then conducted to analyze the helical propensity of the peptides. The studies were carried out in PBS buffer, and the spectra were recorded between 190 and 260 nm. For comparison, the natural peptide N1 was included as a control. As shown in Figure 6, N1 exhibited double minima at 204 and 222 nm, indicating that it adopted the α -helical conformation. In contrast, all our Dsulfono- γ -AA peptides showed a single minimum of \sim 210 to 215 nm, revealing their right-handed helical conformation (it should be noted that the CD signatures of the helical α -peptide and Dsulfono-γ-AA peptides are completely different due to their distinct molecular scaffolds), which demonstrated their ability to mimic the E2 α -1 helix. Besides, a more pronounced minimum of M1-S1 at 215 nm compared to that of the linear peptide M1 or stapled peptide M1-S2 suggested that M1-S1 adopted a more well-defined helical structure in solution.

Peptide Aggregation Propensity. The aggregation of peptides could be a hurdle for developing peptides with therapeutic activities. We thus first evaluated the peptide aggregation propensity of M1–S1 and M1–S2 by ¹H NMR. As shown in Figure S4, the spectra of M1–S1 or M1–S2 showed

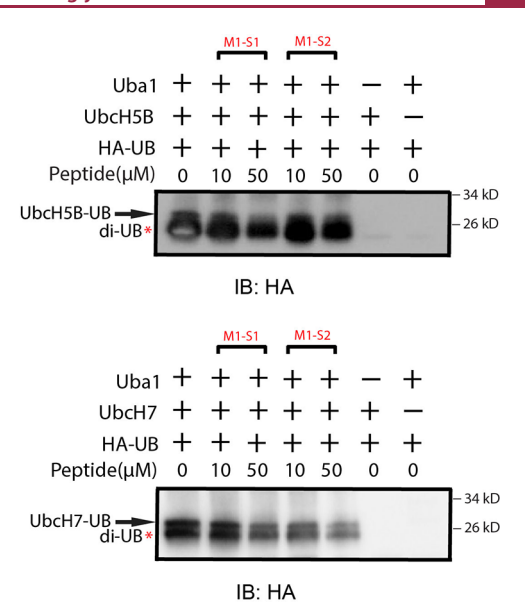


Figure 5. Peptides M1–S1 and M1–S2 inhibit UB transfer from E1 to E2 enzymes, UbcH5B and UbcH7. HA-UB was used for UB transfer between E1 and E2 and the formation of the E2–UB conjugate was probed using an anti-HA antibody. di-UB, UB dimer formed by the E1 and E2 enzymes.

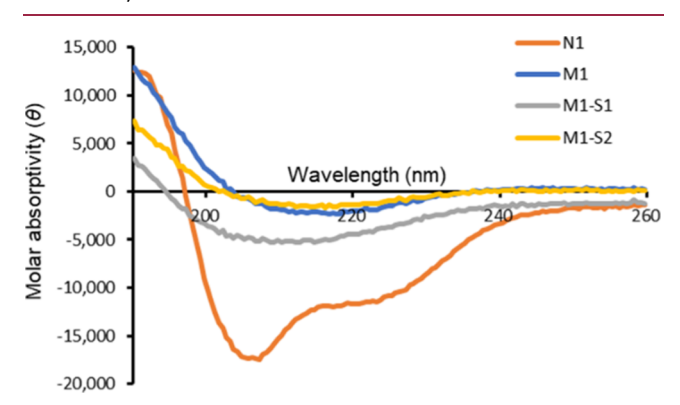


Figure 6. CD spectra of the linear D-sulfono γ -AA peptide M1, stapled D-sulfono γ -AA peptides M1–S1 and M1–S2, and control peptide N1, as measured at 100 μ M, room temperature in PBS buffer.

a practically unchanged general appearance within 24 h. A significant signal shift happened only after 10 days, which indicates that although our peptide aggregation increased with the time, it is insignificant at the experimental condition. We also tested the effect of the detergent or salt on the peptide aggregation. When we incubated the FITC-labeled peptide M1-S1 or M1-S2 in PBS buffer with 1% F68, the fluorescence intensities of the peptides were stable with the increasing time, while the fluorescence intensities of the peptides diminished dramatically when they were in PBS buffer without 1% F68 (Figure S4c). This suggests that the aggregation of the peptides was insignificant in the presence of the detergent. Since our binding and functional assays were carried out in the presence of the detergent, we concluded that the designed γ -AA peptides were not prone to aggregation.

Non-specific Membrane Disruption Assays. We performed a hemolytic assay of peptides M1-S1 or M1-S2 against human red blood cells (hRBCs) to rule out the potential side effect of the peptides in disrupting cell membranes. As shown in Figure S5a, our peptides did not disrupt the red blood cell

membrane up to a concentration of 400 μ M. We then conducted a membrane disruption assay on HEK 293 cells by imaging the cells using confocal microscopy. We incubated the peptides with HEK293 cells for 24 h and then stained the cells with 4′,6-diamidino-2-phenylindole (DAPI) and propidium iodide (PI). DAPI is a cell-permeable blue dye regardless of cell viability, and PI is a red dye that only gets into cells when the cell membranes are disrupted. We found no red fluorescence in the PI channel after treating the cells with up to a 100 μ M concentration of the peptides (Figure \$5b), suggesting the peptides would not disrupt the mammalian cell membranes.

Cell Permeability Assays. In order to evaluate cell uptake, we incubated HEK 293 cells with different concentrations of each FITC-labeled peptide, followed by confocal imaging. The peptides we designed showed an excellent cell uptake under all tested concentrations. The results are shown in Figure S6.

Enzymatic Stability and Serum Stability Study. A distinctive characteristic of our peptidomimetics compared with canonical peptides is their remarkable resistance to enzymatic degradation. To assay the stability of the γ-AA peptides in the presence of a protease, we incubated them with 0.1 mg/mL pronase at 37 °C for 24 h. High-performance liquid chromatography (HPLC) and mass spectrometry (MS) of the peptides before and after the exposure to pronase showed that the peptides are resistant to protease cleavage (Figure S7). We also incubated the γ-AA peptides in the human serum for 24 h and confirmed their stability (Figure S8). The superior stability of our sulfono-γ-AA peptide-based peptidomimetics potentiates their use as therapeutic agents.

DISCUSSION

This work demonstrated that α -helical γ -AA peptides with strategically positioned side chains can compete with the native N-terminal helix of the E2 enzyme as an essential component of E1-E2 interaction. By blocking the PPIs between E1 and E2, the designed γ -AA peptides with staples for enforcing an α helical confirmation can inhibit UB transfer through the cascade enzymes and suppress protein ubiquitination in the cell. So far, several E1 inhibitors targeting UB activation by Uba1 have been developed, including TAK-243, largazole, and PYR-41.¹¹ TAK-243 is a mechanism-based inhibitor that reacts with the Cterminal Gly of UB while it is bound to the catalytic Cys residue of E1 through a thioester bond. The resulting UB-TAK-243 conjugate would occupy the UB and ATP-binding site of Uba1 and inhibit its activation of more UB molecules. 47,48 Largozole is a macrocyclic marine natural product that inhibits UB condensation with ATP at the E1 active site to form UBadenylate conjugates so that UB cannot be activated to form a thioester conjugate with the $\rm E1.^{49,50}$ PYR-41 forms a covalent adduct with the catalytic Cys residue of Uba1 to block the formation of the E1-UB conjugate. 51 These inhibitors all target UB activation and formation of E1-UB thioester conjugates, and there is less development of inhibitors targeting the E1-E2 interface to block UB transfer through the cascade enzymes. It was found that short peptides identified by phage selection to mimic the interaction of UB with Uba1 can be activated by Uba1 for the formation of thioester conjugates with E2 and HECT E3s to block UB transfer to the cascade enzymes.⁵² Recently, Walensky's group reported a stapled peptide that would mimic the binding of N-terminal helix of E2 with Uba1. 46 The study demonstrated the activity of the stapled peptide inhibiting protein ubiquitination in reconstituted reactions in vitro.

However, unnatural peptidic foldamers targeting the same PPI interface have not been reported before.

The sulfono- γ -AA peptide, as a new class of helical foldamers, was successfully employed to mimic the protein helical domain and modulate a series of medicinally relevant PPIs. In this study, we employed the strategy of right-handed D-sulfono-γ-AA peptide helical foldamers to mimic the N-terminal α 1-helix of E2 on the basis of the modeled structure of E2 bound to the UFD domain of E1. As the most critical residues of the E2 α 1 helix were involved in binding with E1, a few D-sulfono- γ -AA peptides with Lys side chains at 3a and 5a were designed to reproduce the interaction of the K5 and K9 residues in the native N-terminal helix of E2 with the binding interface of E1. For side chains of Dsulfono-γ-AA peptides not directly involved in the interaction with E1, we designed residues to facilitate the corresponding interactions and contribute to the stability and cell permeability of the designed peptides. The design was considerably successful as the stapled peptidomimetics, M1-S1 and M1-S2, were discovered and demonstrated excellent inhibitory activity toward the ubiquitination cascade.

Overall, our work designed a few stapled sulfono- γ -AA peptides to block the PPI at the E1–E2 interface and verified the activities of designed foldameric inhibitors in suppressing the ubiquitination of E3 substrate proteins in the cell. We have thus developed a new peptidomimetic scaffold with proven cellular activities to expand the drug discovery platform targeting UB transfer for the treatment of various diseases, including cancer and neurodevelopment and degenerative diseases. Since the cascade enzyme for the transfer of UB and UB-like (UBL) proteins such as SUMO and Nedd8 share similar E1–E2 interfaces, we envision that the γ -AA peptides can be further developed to target the transfer of UBL proteins in the cell. $^{53-56}$

■ CONCLUSIONS

We have successfully designed D-sulfono- γ -AA peptide-based helical foldamer mimetics of the N-terminal α -helix of E2. Applying an activity screening and structure optimization workflow, we identified stapled peptidomimetics M1–S1 and M1–S2 as the most potent inhibitors of Uba1. In a panel of complemental assays, we confirmed that they compete with E2s in binding with Uba1 to disrupt the UB transfer reaction. Furthermore, the CD measurements and stability study also suggested that our peptidomimetics adopt stable right-handed helical conformations with a remarkable enzymatic resistance. Thus, our design of sulfono- γ -AA peptides has provided a useful strategy for the development of peptidomimetics to inhibit UB transfer cascades in the cell.

■ EXPERIMENTAL SECTION

Reagents. Fmoc-protected amino acids were purchased from Chem-Impex (Wood Dale, IL). Rink amide MBHA resin (loading 0.4 mmoL/g) was used for the solid-phase synthesis of D-sulfono-γ-AA peptides and was purchased fro GL Biochem. All solvents and other chemical reagents used for building blocks synthesis were obtained from commercial suppliers and used without purification unless otherwise indicated. The D-sulfono-γ-AA peptides were purified and analyzed on a Waters Breeze 2 HPLC system installed with both an analytic module (1 mL/min) and a preparative module (16 mL/min) by employing a method using a 5–100% linear gradient of solvent B [0.1% trifluoroacetic acid (TFA) in MeCN] in solvent A (0.1% TFA in H₂O) over 45 min, followed by 100% solvent B over 5 min. All compounds are >95% pure according to analytical HPLC. The molecular weight of each peptide was confirmed by high-resolution mass spectrometry (HRMS) obtained from an Agilent 6220 using

electrospray ionization time-of-flight (ESI-TOF). 1 H NMR and 13 C NMR spectra were recorded at 150 MHz using TMS as the internal standard. CDCl₃ or DMSO- d_6 was used as the solvent. The following abbreviations are used to describe peak pattens where appropriate: br = broad, s = singlet, d = doublet, t = triplet, q = quartet, and m = multiplet. Coupling constants (J) are reported in Hertz (Hz).

XL1 Blue cells were obtained from Agilent Technologies (Santa Clara, CA, USA). BL21 (DE3) pLysS chemical competent cells were obtained from Invitrogen for protein expression. pET-15b and pET-28a plasmids for protein expression were from Novagen (Madison, WI, USA). Uba1, UbcH5b, the full-length proteins of CHIP, UB, and CDK4 were expressed from pET28a-Uba1, pET15b-UbcH5b, fulllength pET28a-Flag-CHIP, pET15b-UB, and pET28a-CDK4 plasmids, respectively. HEK 293T cells and HEK 293 cells were purchased from American Tissue Culture Collection (ATCC) and cultured in highglucose Dulbecco's modified Eagle medium (DMEM) (Life Technologies, Carlsbad, CA, USA, 11965092) with 10% (v/v) fetal bovine serum (FBS) (Life Technologies, 11965092). The anti-CHIP antibody (sc-133066), anti-UB antibody (sc-8017), anti-CDK4 antibody (sc-23896), and anti- β -actin (sc-47778) were obtained from Santa Cruz Biotechnology. These antibodies were diluted between 500- and 1000fold to probe the western blots. The anti-Flag M2 antibody was purchased from Sigma-Aldrich and was diluted 2000-fold for western blotting. The DAPI and PI were also purchased from Sigma-Aldrich. hRBCs were obtained from the Moffitt Cancer Center in Tampa.

Synthesis of D-Sulfono-*γ***-AA Building Blocks.** The sulfono-*γ*-AA building blocks were synthesized based on a previous report, as shown in Figure S9. Among them, building blocks 1–3 and 6 were synthesized based on route A, building blocks 4 and 5 were synthesized based on route B, and building block 7 was synthesized based on route C.

(*R*)-*N*-(2-((((9*H*-Fluoren-9-yl)methoxy)carbonyl)amino)-5-(tertbutoxy)-5-oxopentyl)-*N*-(isobutylsulfonyl)glycine (*2*). 1 H NMR (600 MHz, CDCl₃): δ 7.75 (d, J = 8.0 Hz, 2H), 7.60 (t, J = 6.8 Hz, 2H), 7.39 (t, J = 7.3 Hz, 2H), 7.32 (d, J = 7.4 Hz, 2H), 5.37 (d, J = 8.6 Hz, 1H), 4.77–4.51 (m, 1H), 4.53–4.37 (m, 1H), 4.37–4.18 (m, 3H), 4.12–4.01 (m, 1H), 3.95–3.77 (m, 1H), 3.39 (dd, J = 14.7, 9.1 Hz, 1H), 3.29 (dd, J = 14.7, 5.2 Hz, 1H), 3.07–2.90 (m, 2H), 2.42–2.23 (m, 3H), 1.96–1.82 (m, 1H), 1.74–1.58 (m, 1H), 1.44 (s, 9H), 1.08 (dd, J = 6.7, 3.3 Hz, 6H). 13 C NMR (151 MHz, CDCl₃): δ 173.2, 172.2, 157.2, 143.9, 141.4, 127.8, 127.2, 125.4, 120.1, 81.2, 67.3, 60.5, 51.0, 48.7, 47.5, 47.2, 31.9, 28.2, 24.9, 22.7, 22.7. HRMS (ESI) ([M + H]⁺) calcd for C_{30} H₄₁N₂O₈S, 589.2584; found, 589.2590.

(*S*)-*N*-(*2*-(((()⁶*H*-Fluoren-9-yl))methoxy)carbonyl)amino)-3-(tertbutoxy)propyl)-*N*-(isobutylsulfonyl)glycine (*6*). ¹H NMR (600 MHz, CDCl₃): δ 7.76 (d, J = 7.5 Hz, 1H), 7.67–7.56 (m, 1H), 7.47–7.35 (m, 2H), 7.35–7.28 (m, 1H), 5.54 (d, J = 8.3 Hz, 1H), 4.46–4.36 (m, 1H), 4.35–4.28 (m, 1H), 4.27–4.20 (m, 1H), 4.17–4.08 (m, 1H), 3.99–3.86 (m, 1H), 3.60–3.47 (m, 1H), 3.47–3.36 (m, 1H), 2.99 (d, J = 6.6 Hz, 1H), 2.37–2.23 (m, 1H), 1.19 (s, 6H), 1.09 (d, J = 6.0 Hz, 5H). ¹³C NMR (151 MHz, CDCl₃): δ 172.7, 156.8, 143.9, 141.4, 127.8, 127.3, 125.4, 120.1, 73.8, 67.3, 61.3, 60.3, 49.3, 48.9, 48.1, 47.2, 27.6, 24.9, 22.8. HRMS (ESI) ([M + H]⁺) calcd for C₂₈H₃₉N₂O₇S, 547.2478; found, 547.6481.

(*R*)-*N*-(2-((((9*H*-Fluoren-9-yl)methoxy)carbonyl)amino)-6-((2-nitrophenyl)sulfonamido)hexyl)-*N*-(methylsulfonyl)glycine (7). 1 H NMR (600 MHz, DMSO): δ 12.85 (s, 1H), 8.06 (t, J = 5.7 Hz, 1H), 8.02–7.93 (m, 2H), 7.91–7.81 (m, 4H), 7.67 (t, J = 6.9 Hz, 2H), 7.47–7.35 (m, 2H), 7.31 (t, J = 7.4 Hz, 2H), 7.11 (d, J = 9.1 Hz, 1H), 4.37–4.28 (m, 2H), 4.20 (t, J = 6.8 Hz, 1H), 3.95 (s, 2H), 3.63–3.50 (m, 1H), 3.22 (dd, J = 14.5, 5.3 Hz, 1H), 3.08 (dd, J = 14.5, 8.7 Hz, 1H), 2.91 (s, 3H), 2.89–2.79 (m, 2H), 1.46–1.29 (m, 3H), 1.26–1.19 (m, 2H). 13 C NMR (151 MHz, DMSO): δ 170.8, 155.9, 147.8, 143.9, 140.7, 133.9, 132.8, 132.6, 129.4, 127.6, 127.0, 125.1, 124.3, 120.1, 65.1, 51.1, 49.5, 48.3, 46.8, 42.6, 31.2, 29.0, 22.4, 20.8. HRMS (ESI) ([M + H]⁺) calcd for C_{30} H₃₅N₄O₁₀S₂, 675.1795; found, 675.1793.

Others are characterized in our previous work.³⁷

Preparation of the E2 Alpha-1 Helix. The synthesis of the E2 alpha-1 helix was carried out on 200 mg of Rink amide resin (0.4 mmoL/g) at room temperature. A scheme could be found in Figure

S10. Specifically, the resin was soaked in dimethylformamide (DMF) for 10 min, and then, the Fmoc group was removed by 20% piperidine in DMF solution (15 min ×2). After a thorough wash with dimethyl carbonate (DMC) and DMF, the Fmoc-protected amino acid (2 equiv) was coupled to the resin under the condition of DIC (4 equiv) and HOBt (4 equiv) in DMF for 4 h. Then, the resin was washed with DMF and dichloromethane (DCM) and treated with 20% piperidine in DMF solution again, followed by coupling with the next amino acid. This reaction cycle was repeated until the desired peptides were synthesized. After removing the last Fmoc group, the N-terminus of the sequence was capped with acetic anhydride (2 mL) in pyridine (4 mL) two times. Then, the peptides were cleaved from the resin by the solution of TFA/DCM (4 mL, 1:1, v/v) and purified using the Waters HPLC system.

Preparation of Linear D-Sulfono-*γ***-AA Peptides.** The synthesis of linear D-sulfono-γ-AA peptides was carried out on 200 mg of Rink amide resin (0.4 mmoL/g) at room temperature. A scheme could be found in Figure S10. Specifically, the resin was soaked in DMF for 10 min, and then, the Fmoc group was removed by 20% piperidine in DMF solution (15 min ×2). After a thorough wash with DMC and DMF, the sulfono- γ -AA building block (2 equiv) was coupled to the resin under the condition of DIC (4 equiv) and HOBt (4 equiv) in DMF for 4 h. Then, the resin was washed with DMF and DCM and treated with 20% piperidine in DMF solution again, followed by coupling with the next sulfono-γ-AA building block. These cycles were repeated until the desired sulfono- γ -AA peptides were synthesized. After removing the last Fmoc group, the N-terminus of the sequence was capped with acetic anhydride (2 mL) in pyridine (4 mL) two times. Then, the peptides were cleaved from the resin by the solution of TFA/DCM (4 mL, 1:1, v/v) and purified using the Waters HPLC system.

Preparation of Stapled D-Sulfono-*γ***-AA Peptides.** The synthesis of stapled D-sulfono-γ-AA peptides was carried out on 250 mg of Rink amide resin (0.4 mmoL/g) at room temperature. As shown in Figure S10, after capping the N-terminus of the sequence with acetic anhydride, the o-NBS was removed by DBU (10 equiv) and 2-mercaptoethanol (5 equiv) in DMF for 30 min, followed by the addition of a solution of terephthaloyl chloride (1 equiv) and N_iN_i -diisopropylethylamine (DIPEA) (10 equiv) in DCM, and after the mixture was shaken for 1 h, the stapled peptides were cleaved from the resin by the solution of TFA/DCM (4 mL, 1:1, v/v) and purified using the Waters HPLC system.

Preparation of the FITC-Labeled E2 Alpha-1 Helix and D-Sulfono- γ -AA Peptides. After attaching the last amino acid or sulfono- γ -AA building block, the Fmoc protecting group was then removed, and Fmoc-protected β -Ala-OH (2 equiv), DIC (4 equiv), and HOBt (4 equiv) were added. The mixture was shaken for 2 h, and then, the Fmoc group was removed, and FITC (1.2 equiv) in 3 mL of DMF and DIPEA (10 equiv) were added to the resin. After shaking overnight, the resin was washed with DMF and DCM, and then, the FITC-labeled peptide was cleaved by 1:1 (v/v) DCM/TFA. The crude was purified using the Waters HPLC system, and the detailed structures can be found in Table S1.

FP Assays to Measure the Binding Affinity of the E2 Alpha-1 Helix or D-Sulfono- γ -AA Peptides to Uba1, UbcH5A, and CHIP. The binding affinity ($K_{\rm d}$) of the peptides were measured by FP. Briefly, a constant amount of the 50 nM FITC-labeled peptide was incubated with a serial dilution of protein in binding buffer [20 mM HEPES pH 7.4, 50 mM NaCl, 5 mM dithiothreitol (DTT), 1% F68]. The $K_{\rm d}$ values was calculated using the following equation, in which the $L_{\rm st}$ and x refer to the concentrations of the peptide and protein, respectively.

Fluorescent Bead Binding Assay. Each His-tagged protein (10 μ g) was incubated with Ni-NTA agarose beads (50 μ L) (Invitrogen, catalog no. R90110) in PBS (1% F68) for 30 min, respectively. The beads were then incubated with the FITC-labeled peptide (10 μ M) for 30 min, isolated by benchtop centrifugation (2000g), resuspended in PBS for plating in a 96-well plate format, and imaged using an Olympus FV1000 MPE multiphoton laser scanning microscope.

In Vitro **UB Transfer Assays with Different E2 Enzymes. UB** transfer assays were conducted in a 50 μ L reaction buffer supplemented with 50 mM Tris, 5 mM MgCl₂, 5 mM ATP, and 1 mM DTT. A 10 or 50 μ M concentration of each peptide was incubated with 0.5 μ M wt

Uba1, 0.5 μ M wt UbcHSb, or UbcH7 at 37 °C for 30 min before 1 μ M wt UB was added to initiate the UB transfer reaction. The reactions were incubated for another 30 min h at 37 °C and then quenched by boiling in the sample loading buffer of sodium dodecyl sulfate—polyacrylamide gel electrophoresis (SDS-PAGE) without DTT for 5 min and analyzed by SDS-PAGE and western blotting probed with the anti-HA antibody.

Circular Dichroism. The CD spectra of peptides were measured in PBS at a concentration of 100 μ M by using an Aviv 215 CD spectrometer with a 1 mm path length quartz cuvette. Ten scans were averaged for each sample, and three independent experiments were conducted. The final spectra were normalized by subtracting the average blank spectra. Molar ellipticity $[\theta]$ (deg·cm²·dmol⁻¹) was calculated using the following equation

$$[\theta] = \theta_{\rm obs}/(n \times I \times c \times 10)$$

where $\theta_{\rm obs}$ is the measured ellipticity in millidegree, n is the number of side groups, I is the path length in centimeters (0.1 cm), and c is the centration of the peptide in molar units.

Peptide Aggregation Assay. ¹H NMR experiments were performed at 25 °C on a Varian Unity Inova 600 MHz spectrometer with the peptide concentration of 1 mM in D_2O . The samples were gently agitated, by manual swirling, until the solution appeared visually homogeneous, and 450 μ L of each sample was transferred to disposable 5 mm NMR tubes. The spectra were then acquired at different times.

For the detergent assays, we dissolved the peptides in $1 \times PBS$ buffer with or without 1% F68 as a detergent to a final concentration of 1 mM, and then, the fluorescence intensities of the peptides were obtained by using a microplate reader.

Cell Permeability Assay. HEK 293 cells were cultured in 6-well plates and allowed to attach to the bottom of the plate overnight. Then, appropriate amounts of FITC-labeled peptides dissolved in DMEM were added to the cells to final concentrations of 1, 10, and 20 μ M. The cells were incubated with the peptides for 4 h at 37 °C and 5% CO₂. After incubation, cells were washed three times with PBS and stained with DAPI (10 μ g/mL) for 10 min, and then, it was washed with PBS twice and fixed with methanol for 5 min. They are then washed two times with PBS and imaged using an Olympus FV1000 MPE multiphoton laser scanning microscope.

Hemolytic Assay. Hemolytic activity was determined by incubating suspensions of hRBCs with serial dilutions of each peptide. hRBCs were rinsed several times in PBS, followed by centrifugation at 4 °C/700g for 10 min. Then the supernatants were removed, and the remaining hRBCs were diluted with PBS buffer in a 1:20 ratio. Then, 50 μ L of the diluted hRBC was added to the prepared 96-well microplate, which contains different concentrations of each peptide. The PBStreated hRBC is the negative control, and hRBC treated with 1% Triton was the positive control. Then, the 96-well microplate was incubated at 37 °C for 1 h and centrifuged at 4 °C/3500 rpm for 10 min. 100 μ L of PBS buffer was added to a new 96-well microplate, and 30 μ L of the supernatant from the centrifuged solution was transferred to the new 96-well microplate. The absorbance was measured at 540 nm. The hemolysis percentage was calculated as (Abbs_{Sample} - Abbs_{buffer})/ $(Abbs_{Triton} - Abbs_{buffer}) \times 100\%$, where Abbs is the absorbance detection at 540 nm. The experiment was performed in duplicate and repeated independently three times.

Membrane Disruption Assay. HEK 293 cells were cultured in sixwell plates and allowed to attach to the bottom of the plate overnight. Then, it was digested with 0.25% Trypsin and transferred to a centrifuge tube, followed by the centrifugation at 800 rpm for 5 min. The supernatant was removed, and the cells were washed with PBS twice. Then, the appropriate amounts of peptides dissolved in DMEM were added to the cells to final concentrations of 10, 50, and 100 μ M. The cells were incubated with the peptides for 1 h at 37°. After the incubation, the tube was centrifuged, and the supernatant was removed. The cells were washed three times with PBS and stained with PI (10 μ g/mL) for 10 min. After centrifugation and removing the supernatant, the cells were washed with PBS twice and fixed with methanol for 5 min. Then, it was stained with DAPI (10 μ g/mL) for 10 min, followed by washing with PBS twice, and transferred to a new six-well plates. They

are then washed twice with PBS and imaged using an Olympus FV1000 MPE multiphoton laser scanning microscope.

Enzymatic Stability Study. A 0.1 mg/mL concentration of the peptide was incubated with 0.1 mg/mL pronase in 100 mM ammonium bicarbonate buffer (pH 7.8) at 37 °C for 24 h. The reaction mixture was concentrated in a speed vacuum to remove the water and ammonium bicarbonate. The remains were dissolved in 100 μ L of H₂O/CH₃CN (1:1, v/v) and analyzed using a Waters analytical HPLC system with a 1 mL/min flow rate and a 5–100% linear gradient of solvent B (0.1% TFA in acetonitrile) in A (0.1% TFA in water) over the duration of 50 min. The UV detector was set to 215 nm.

Serum Stability Assay. The serum stabilities of peptides were determined in 50% (v/v) aqueous pooled serum from human male AB plasma (Sigma-Aldrich, Milan, Italy). 1 mg of the peptide was dissolved in 50 μ L of H₂O and then diluted in serum and incubated at 37 °C for 24 h. Then, 100 μ L of the solution was added to 100 μ L of CH₃CN on ice for 15 min and was centrifuged at 4 °C for 10 min. The supernatant was then analyzed using a Waters analytical HPLC system with a 1 mL/min flow rate and a 5–100% linear gradient of solvent B (0.1% TFA in acetonitrile) in A (0.1% TFA in water) over the duration of 50 min. The UV detector was set to 215 nm.

Proteins Expression from Recombinant pET Plasmids. Recombinant pET plasmids for the expression of Uba1, UbcH5B, CHIP full length, UB, and CDK4 were transformed into BL21 cells and cultured in 2XYT broth with kanamycin (70 mg/mL) at 37 °C until the OD₆₀₀ value of the media is within the range of 0.6–0.8. 1 mM IPTG was added to the cell culture to induce the expression, and the cell culture was incubated overnight under 15 °C with agitation before the cells were harvested by centrifugation (5000 rpm, 4 °C, 30 min). Cells were resuspended in 5-10 mL of lysis buffer (50 mM NaH₂PO₄, 300 mM NaCl, 10 mM imidazole, pH 8.0) with the addition of 2 mg/mL lysozyme (Alfa Aesar), and the mixture was incubated on ice for 30 min. The cell resuspension was sonicated on ice, the resulting cell lysate was centrifuged (10,000 rpm, 4 °C, 25 min), and the supernatant was collected to bind with Ni-NTA beads (BioVision, cat. 6562-100) overnight at 4 °C. The protein was purified using a gravity-flow column with washes by 20 mL of lysis buffer (50 mM NaH₂PO₄, 300 mM NaCl, 5 mM imidazole, pH 8.0) once and 20 mL of wash buffer (50 mM NaH₂PO₄, 300 mM NaCl, 20 mM imidazole, pH 8.0) twice, followed by an elution with 5 mL of elution buffer (50 mM NaH₂PO₄, 300 mM NaCl, 250 mM imidazole, pH 8.0). The eluted protein solution was further dialyzed overnight at 4 °C in a dialysis buffer (50 mM Tris, 150 mM NaCl, 1 mM DTT, pH 7.5) and concentrated. Then, the concentration was measured using a Bradford assay according to the vendor's protocol (Bio-Rad). The success of the expression was confirmed via western blotting and Coomassie staining of the SDS gel, and the yield of the purified protein was assessed using a standard Bradford assay and taken as the total protein concentration.

In Vitro Assay to Measure the Effect of the D-Sulfono-γ-AA Peptides on CHIP Self-Ubiquitination and CDK4 Ubiquitina**tion.** All assays were set up in 50 μ L of reaction buffer supplemented with 50 mM Tris, 5 mM MgCl₂, 5 mM ATP, and 1 mM DTT. A 10 or 50 μ M concentration of each peptide was incubated with 1.0 μ M wt Uba1, 1.0 μ M wt UbcH5B, and 0.5 μ M wt N-terminal Flag-tagged fulllength CHIP at 37 °C for 30 min before 5 μ M wt UB was added to start the UB transfer reaction. The reactions were incubated for another 1 h at 37 °C and then quenched by boiling in the sample loading buffer of SDS-PAGE with DTT for 5 min and analyzed by SDS-PAGE and western blotting probed with the anti-Flag antibody. In the CDK4 ubiquitination assay, CDK4 was added to the reaction mixture (Uba1, UbcH5B, CHIP, and UB) for a 2 h reaction at 37 °C and then quenched by boiling in the sample loading buffer of SDS-PAGE with DTT for 5 min and analyzed by SDS-PAGE and western blotting probed with anti-CDK4.

In Cell-Based Assay to Measure the Inhibitory Effect of M1–S1 and M1–S2 on CDK4 Ubiquitination. HEK293T cells were preincubated with each peptide at 0, 10, and 50 μ M for 14 h and with 0.5 μ M MG132 for an additional 12 h. Cells were then washed twice with ice-cold PBS, pH 7.4, and 1 mL of ice-cold RIPA buffer was added and incubated with the cells at 4 °C for 10 min. The cells were disrupted

by repeated aspiration through a 21-gauge needle to induce cell lysis, and the cell lysate was transferred to a 1.5 mL tube. The cell debris was pelleted by centrifugation at 13,000 rpm for 20 min at 4 °C, and the supernatant was transferred to a new tube and precleared by adding 1.0 µg of the appropriate control IgG (normal mouse or rabbit IgG corresponding to the host species of the primary antibody). 20 μ L of suspended Protein A/G PLUS-agarose was added to the supernatant, and the incubation was continued for 30 min at 4 °C. After this, the cell lysate containing 2 mg of the total protein was transferred to a new tube, and 30 μ L (i.e., 6 μ g) of the primary antibody specific for CDK4 was added. The incubation was continued for 1 h at 4 $^{\circ}$ C, and 40 μ L of resuspended Protein A/G PLUS-Agarose was added. The tubes were capped and incubated at 4 °C on a rocking platform overnight. The next day, the agarose beads were pelleted by centrifugation at 350g for 5 min at 4 °C. The beads were then washed three times, each time with 1.0 mL of PBS. After the final wash, the beads were resuspended in 40 μ L of 1× Laemmli buffer with β -mercaptoethanol. The samples were boiled for 5 min and analyzed by SDS-PAGE and western blotting probed with an anti-UB antibody.

ASSOCIATED CONTENT

Supporting Information

The Supporting Information is available free of charge at https://pubs.acs.org/doi/10.1021/acs.jmedchem.2c01459.

Schematic illustration of the structure of the sulfono- γ -AA peptide; schematic illustration of the procedure to synthesize peptides and building blocks; analytic HPLC traces of enzymatic and serum stability; structures of FITC-labeled peptides; HRMS of all peptides and FITC-labeled peptides; HPLC traces of all compounds; copies of NMR spectra of building blocks; structural information of the sulfono- γ -AA peptide; cartoon mode of the alpha-1 helix of Ubc1 and sulfono- γ -AA peptide; binding affinity of linear peptide M1 to Uba1; peptide aggregation assays; non-specific membrane disruption assays; and confocal imaging of HEK 293T cells treated with peptides M1–S1 and M1–S2 at 1, 10, and 20 μ M (PDF)

SMILES of all peptides and FITC-labeled peptides (CSV)

AUTHOR INFORMATION

Corresponding Authors

Jianfeng Cai − Department of Chemistry, University of South Florida, Tampa, Florida 33620, United States; o orcid.org/0000-0003-3106-3306; Email: jianfengcai@usf.edu

Jun Yin — Department of Chemistry and Center for Diagnostics & Therapeutics, Georgia State University, Atlanta, Georgia 30303, United States; orcid.org/0000-0002-4803-7510; Email: junyin@gsu.edu

Bo Huang – Department of Chemistry, University of South Florida, Tampa, Florida 33620, United States; orcid.org/0000-0001-6196-5373; Email: bohuang@usf.edu

Authors

Li Zhou – Department of Chemistry and Center for Diagnostics & Therapeutics, Georgia State University, Atlanta, Georgia 30303, United States; oorcid.org/0000-0002-2815-9430

In Ho Jeong – Department of Chemistry and Center for Diagnostics & Therapeutics, Georgia State University, Atlanta, Georgia 30303, United States

Songyi Xue – Department of Chemistry, University of South Florida, Tampa, Florida 33620, United States

Menglin Xue — Department of Chemistry, University of South Florida, Tampa, Florida 33620, United States Lei Wang — Department of Chemistry, University of South Florida, Tampa, Florida 33620, United States

Sihao Li – Department of Chemistry, University of South Florida, Tampa, Florida 33620, United States

Ruochuan Liu – Department of Chemistry and Center for Diagnostics & Therapeutics, Georgia State University, Atlanta, Georgia 30303, United States

Geon Ho Jeong – Department of Chemistry and Center for Diagnostics & Therapeutics, Georgia State University, Atlanta, Georgia 30303, United States

Xiaoyu Wang — Department of Chemistry and Center for Diagnostics & Therapeutics, Georgia State University, Atlanta, Georgia 30303, United States

Complete contact information is available at: https://pubs.acs.org/10.1021/acs.jmedchem.2c01459

Author Contributions

L.Z and I.H.J. contributed to the work equally. J.Y., J.C., and B.H. designed the experiments. B.H. prepared all the peptidomimetics, conducted specific binding assays, and tested the enzymatic stability and serum stability of stapled peptides and CD spectra. L.Z. and I.H.J. assayed the ligand activities in reconstituted ubiquitination reactions. L.Z. performed the cellular assay of stapled peptidomimetics. S.X. synthesized some peptides. M.X. helped with the fluorescence microscopybased qualitative binding assay. L.W. and S.L. helped with the preparation of building blocks. R.L. and G.H.J. expressed UB transferring enzymes for *in vitro* assays. X.W. helped with ubiquitin transfer assays. B.H., L.Z., I.H.J, J.Y., and J.C. analyzed the data and interpreted the results. J.Y., B.H., L.Z., and J.C. wrote and revised the manuscript. All authors reviewed and approved the final version of the manuscript.

Notes

The authors declare no competing financial interest.

ACKNOWLEDGMENTS

This work was supported by grants from NIH (R01AG056569 and R01AI152416 to J.C. and R01GM104498 to J.Y.) and NSF (1710460 and 2109051 to J.Y.)

ABBREVIATIONS

ACN, acetonitrile; CDK4, cyclin-dependent kinase 4; CHIP, carboxy terminus of Hsc70-interacting protein; CHX chase, cycloheximide chase; DAPI, 4′,6-diamidino-2-phenylindole; DCM, dichloromethane; DIPEA, N,N-diisopropylethylamine; DTT, dithiothreitol; FITC, fluorescein isothiocyanate; MG132, carbobenzoxy-Leu-Leu-leucinal; PI, propidium iodide; PPIs, protein—protein interactions; SDS-PAGE, sodium dodecyl sulfate—polyacrylamide gel electrophoresis; TFA, trifluoroacetic acid; UB, ubiquitin; Uba1, ubiquitin-like modifier activating enzyme 1; Ubc1, ubiquitin-conjugating enzyme E2; UbcHSb, ubiquitin-conjugating enzyme HSb; UPS, ubiquitin—proteasome system; γ -AA peptide, γ -substituted-N-acylated-N-aminoethyl peptide

REFERENCES

- (1) Pickart, C. M. Mechanisms underlying ubiquitination. *Annu. Rev. Biochem.* **2001**, *70*, 503–533.
- (2) Hershko, A.; Ciechanover, A. The ubiquitin system. *Annu. Rev. Biochem.* **1998**, *67*, 425–479.
- (3) Mevissen, T. E. T.; Komander, D. Mechanisms of deubiquitinase specificity and regulation. *Annu. Rev. Biochem.* **2017**, *86*, 159–192.

- (4) Komander, D.; Rape, M. The ubiquitin code. *Annu. Rev. Biochem.* **2012**, *81*, 203–229.
- (5) Oh, E.; Akopian, D.; Rape, M. Principles of ubiquitin-dependent signaling. *Annu. Rev. Cell Dev. Biol.* **2018**, *34*, 137–162.
- (6) Lipkowitz, S.; Weissman, A. M. RINGs of good and evil: RING finger ubiquitin ligases at the crossroads of tumour suppression and oncogenesis. *Nat. Rev. Cancer* **2011**, *11*, 629–643.
- (7) Schwartz, A. L.; Ciechanover, A. Targeting proteins for destruction by the ubiquitin system: implications for human pathobiology. *Annu. Rev. Pharmacol. Toxicol.* **2009**, 49, 73–96.
- (8) Bedford, L.; Lowe, J.; Dick, L. R.; Mayer, R. J.; Brownell, J. E. Ubiquitin-like protein conjugation and the ubiquitin-proteasome system as drug targets. *Nat. Rev. Drug Discov.* **2011**, *10*, 29–46.
- (9) Wertz, I. E.; Wang, X. From discovery to bedside: Targeting the ubiquitin system. *Cell Chem. Biol.* **2019**, *26*, 156–177.
- (10) Harrigan, J. A.; Jacq, X.; Martin, N. M.; Jackson, S. P. Deubiquitylating enzymes and drug discovery: emerging opportunities. *Nat. Rev. Drug Discov.* **2018**, *17*, 57–78.
- (11) Barghout, S. H.; Schimmer, A. D. E1 enzymes as therapeutic targets in cancer. *Pharmacol. Rev.* **2021**, *73*, 1–56.
- (12) Teicher, B. A.; Ara, G.; Herbst, R.; Palombella, V. J.; Adams, J. The proteasome inhibitor PS-341 in cancer therapy. *Clin. Cancer Res.* **1999**, *5*, 2638–2645.
- (13) Scott, D. E.; Bayly, A. R.; Abell, C.; Skidmore, J. Small molecules, big targets: drug discovery faces the protein-protein interaction challenge. *Nat. Rev. Drug Discov.* **2016**, *15*, 533–550.
- (14) Gaczynska, M.; Osmulski, P. A. Targeting protein-protein interactions in the ubiquitin-proteasome pathway. *Adv. Protein Chem. Struct. Biol.* **2018**, *110*, 123–165.
- (15) Blaquiere, N.; Villemure, E.; Staben, S. T. Medicinal chemistry of inhibiting RING-type E3 ubiquitin lLigases. *J. Med. Chem.* **2020**, *63*, 7957–7985.
- (16) Jin, J.; Li, X.; Gygi, S. P.; Harper, J. W. Dual E1 activation systems for ubiquitin differentially regulate E2 enzyme charging. *Nature* **2007**, 447, 1135–1138.
- (17) Liu, X.; Zhao, B.; Sun, L.; Bhuripanyo, K.; Wang, Y.; Bi, Y.; Davuluri, R. V.; Duong, D. M.; Nanavati, D.; Yin, J.; Kiyokawa, H. Orthogonal ubiquitin transfer identifies ubiquitination substrates under differential control by the two ubiquitin activating enzymes. *Nat. Commun.* **2017**, *8*, 14286.
- (18) Deshaies, R. J.; Joazeiro, C. A. RING domain E3 ubiquitin ligases. *Annu. Rev. Biochem.* **2009**, *78*, 399–434.
- (19) Ye, Y.; Rape, M. Building ubiquitin chains: E2 enzymes at work. *Nat. Rev. Mol. Cell Biol.* **2009**, *10*, 755–764.
- (20) Rotin, D.; Kumar, S. Physiological functions of the HECT family of ubiquitin ligases. *Nat. Rev. Mol. Cell Biol.* **2009**, *10*, 398–409.
- (21) Lee, I.; Schindelin, H. Structural insights into E1-catalyzed ubiquitin activation and transfer to conjugating enzymes. *Cell* **2008**, 134, 268–278.
- (22) Huang, L.; Kinnucan, E.; Wang, G.; Beaudenon, S.; Howley, P. M.; Huibregtse, J. M.; Pavletich, N. P. Structure of an E6AP-UbcH7 complex: insights into ubiquitination by the E2-E3 enzyme cascade. *Science* 1999, 286, 1321–1326.
- (23) Buetow, L.; Gabrielsen, M.; Anthony, N. G.; Dou, H.; Patel, A.; Aitkenhead, H.; Sibbet, G. J.; Smith, B. O.; Huang, D. T. Activation of a primed RING E3-E2-ubiquitin complex by non-covalent ubiquitin. *Mol. Cell* **2015**, *58*, 297–310.
- (24) Dou, H.; Buetow, L.; Sibbet, G. J.; Cameron, K.; Huang, D. T. BIRC7-E2 ubiquitin conjugate structure reveals the mechanism of ubiquitin transfer by a RING dimer. *Nat. Struct. Mol. Biol.* **2012**, *19*, 876–883
- (25) Xu, Z.; Kohli, E.; Devlin, K. I.; Bold, M.; Nix, J. C.; Misra, S. Interactions between the quality control ubiquitin ligase CHIP and ubiquitin conjugating enzymes. *BMC Struct. Biol.* **2008**, *8*, 26.
- (26) Zhao, B.; Tsai, Y. C.; Jin, B.; Wang, B.; Wang, Y.; Zhou, H.; Carpenter, T.; Weissman, A. M.; Yin, J. Protein engineering in the ubiquitin system: Tools for discovery and beyond. *Pharmacol. Rev.* **2020**, 72, 380–413.

- (27) Zhao, B.; Bhuripanyo, K.; Zhang, K.; Kiyokawa, H.; Schindelin, H.; Yin, J. Orthogonal ubiquitin transfer through engineered E1-E2 cascades for protein ubiquitination. *Chem. Biol.* **2012**, *19*, 1265–1277. (28) Shi, Y.; Teng, P.; Sang, P.; She, F.; Wei, L.; Cai, J. γ -AApeptides: design, structure, and application. *Acc. Chem. Res.* **2016**, *49*, 428–441.
- (29) Huang, B.; Zhou, L.; Liu, R.; Wang, L.; Xue, S.; Shi, Y.; Jeong, G. H.; Jeong, I. H.; Li, S.; Yin, J.; Cai, J. Activation of E6AP/UBE3A-mediated protein ubiquitination and degradation pathways by a cyclic γ-AA peptides. *J. Med. Chem.* **2022**, *65*, 2497–2506.
- (30) Zheng, M.; Li, C.; Zhou, M.; Jia, R.; Cai, F.; She, L.; Wei, S.; Wang, J.; Yu, D.; Wang, L.; Calcul, X.; Sun, X.; Luo, F.; Cheng, Q.; Li, Y.; Wang, J. Discovery pf cyclic peptidomimetic ligands targeting the extracellular domain of EGFR. J. Med. Chem. 2021, 64, 11219–11228.
- (31) Singh, S.; Wang, M.; Gao, R.; Teng, P.; Odom, T.; Zhang, E.; Xu, H.; Cai, J. Lipidated α /sulfono- α -AA heterogeneous peptides as antimicrobial agents for MRSA. *Bioorg. Med. Chem.* **2020**, 28, 115241.
- (32) Wei, L.; Wang, M.; Gao, R.; Fatirkhorani, R.; Cai, J. Antibacterial activity of lipo-α/sulfono-γ-AA hybrid peptides. *Eur. J. Med. Chem.* **2020**, *186*, 111901.
- (33) She, F.; Teng, P.; Peguero-Tejada, A.; Wang, M.; Ma, N.; Odom, T.; Zhou, M.; Gjonaj, E.; Wojtas, L.; Vaart, A.; Cai, J. De novo left-handed synthetic peptidomimetic foldamers. *Angew. Chem., Int. Ed.* **2018**, *57*, 9916–9920.
- (34) Abdulkadir, S.; Li, C.; Jiang, W.; Zhao, X.; Sang, P.; Wei, L.; Hu, Y.; Li, Q.; Cai, J. Modulating angiogenesis by proteomimetics of vascular endothelial growth factor. *J. Am. Chem. Soc.* **2022**, 144, 270–281.
- (35) Sang, P.; Zhang, M.; Shi, Y.; Li, C.; Abdulkadir, S.; Li, Q.; Ji, H.; Cai, J. Inhibition of β -catenin/ B cell lymphoma 9 protein-protein interaction using α -helix-mimicking sulfono- γ -AApeptides inhibitors. *Proc. Natl. Acad. Sci. U.S.A.* **2019**, *116*, 10757–10762.
- (36) Sang, P.; Shi, Y.; Lu, J.; Chen, L.; Yang, L.; Borcherds, W.; Abdulkadir, S.; Li, Q.; Daughdrill, J.; Chen, J. α -Helix -mimicking sulfono- γ -AApeptide inhibitors for P53-MDM2/MDMX protein-protein interactions. *J. Med. Chem.* **2020**, *63*, 975–986.
- (37) Sang, P.; Shi, Y.; Higbee, P.; Wang, M.; Abdulkadir, S.; Lu, J.; Daughdrill, G.; Chen, J.; Cai, J. Rational design and synthesis of right-handed D-sulfono-γ-AApeptide helical foldamers as potent inhibitors of protein-protein interactions. *J. Org. Chem.* **2020**, *85*, 10552–10560.
- (38) Shi, Y.; Sang, P.; Lu, J.; Higbee, P.; Chen, L.; Yang, L.; Odom, T.; Daughdrill, G.; Chen, J.; Cai, J. Rational design of right-handed heterogeneous peptidomimetics as inhibitors of protein-protein interactions. *J. Med. Chem.* **2020**, *63*, 13187–13196.
- (39) Sang, P.; Zhou, Z.; Shi, Y.; Lee, C.; Amso, Z.; Huang, D.; Odom, T.; Nguyen-Tran, V. T. B.; Shen, W.; Cai, J. The activity of sulfono-γ-AApeptide helical foldamers that mimic GLP-1. *Sci. Adv.* **2020**, *6*, No. eaaz4988.
- (40) Olsen, S. K.; Lima, C. D. Structure of a ubiquitin E1-E2 complex: insights to E1-E2 thioester transfer. *Mol. Cell* **2013**, *49*, 884–896.
- (41) Lv, Z.; Rickman, K. A.; Yuan, L.; Williams, K.; Selvam, S. P.; Woosley, A. N.; Howe, P. H.; Ogretmen, B.; Smogorzewska, A.; Olsen, S. K. S. pombe Uba1-Ubc15 Structure Reveals a Novel Regulatory Mechanism of Ubiquitin E2 Activity. *Mol. Cell* **2017**, *65*, 699–714.
- (42) Yuan, L.; Lv, Z.; Adams, M. J.; Olsen, S. K. Crystal structures of an E1-E2-ubiquitin thioester mimetic reveal molecular mechanisms of transthioesterification. *Nat. Commun.* **2021**, *12*, 2370.
- (43) Williams, K. M.; Qie, S.; Atkison, J. H.; Salazar-Arango, S.; Diehl, J.; Olsen, S. K. Structural insights into E1 recognition and the ubiquitin-conjugating activity of the E2 enzyme Cdc34. *Nat. Commun.* **2019**, *10*, 3296.
- (44) Li, X.; Chen, W. D.; Zhang, H. G. Stapled helical peptides bearing different anchoring residues. *Chem. Rev.* **2020**, *120*, 10079–10144.
- (45) Bhuripanyo, K.; Wang, Y.; Liu, X.; Zhou, L.; Liu, R.; Duong, D.; Zhao, B.; Bi, Y.; Zhou, H.; Chen, G.; Seyfried, N. T.; Chazin, W. J.; Kiyokawa, H.; Yin, J. Identifying the substrate proteins of U-box E3s E4B and CHIP by orthogonal ubiquitin transfer. *Sci. Adv.* **2018**, *4*, No. e1701393.
- (46) Cathcart, A. M.; Bird, G. H.; Wales, T. E.; Herce, H. D.; Harvey, E. P.; Hauseman, Z. J.; Newman, C. E.; Adhikary, U.; Prew, M. S.; Oo,

- T.; Lee, S.; Engen, J. R.; Walensky, L. D. Targeting a helix-in-groove interaction between E1 and E2 blocks ubiquitin transfer. *Nat. Chem. Biol.* **2020**, *16*, 1218–1226.
- (47) Misra, M.; Kuhn, M.; Löbel, M.; An, H.; Statsyuk, A. V.; Sotriffer, C.; Schindelin, H. Dissecting the specificity of adenosyl sulfamate inhibitors targeting the ubiquitin-activating enzyme. *Structure* **2017**, 25, 1120–1129.
- (48) Hyer, M. L.; Milhollen, M. A.; Ciavarri, J.; Fleming, P.; Traore, T.; Sappal, D.; Huck, J.; Shi, J.; Gavin, J.; Brownell, J.; Yang, Y.; Stringer, B.; Griffin, R.; Bruzzese, F.; Soucy, T.; Duffy, J.; Rabino, C.; Riceberg, J.; Hoar, K.; Lublinsky, A.; Menon, S.; Sintchak, M.; Bump, N.; Pulukuri, S. M.; Langston, S.; Tirrell, S.; Kuranda, M.; Veiby, P.; Newcomb, J.; Li, P.; Wu, J. T.; Powe, J.; Dick, L. R.; Greenspan, P.; Galvin, K.; Manfredi, M.; Claiborne, C.; Amidon, B. S.; Bence, N. F. A small-molecule inhibitor of the ubiquitin activating enzyme for cancer treatment. *Nat. Med.* **2018**, *24*, 186–193.
- (49) Ungermannova, D.; Parker, S. J.; Nasveschuk, C. G.; Wang, W.; Quade, B.; Zhang, G.; Kuchta, R. D.; Phillips, A. J.; Liu, X. Largazole and its derivatives selectively inhibit ubiquitin activating enzyme (e1). *PLoS One* **2012**, *7*, No. e29208.
- (50) Ungermannova, D.; Parker, S. J.; Nasveschuk, C. G.; Chapnick, D. A.; Phillips, A. J.; Kuchta, R. D.; Liu, X. Identification and mechanistic studies of a novel ubiquitin E1 inhibitor. *J. Biomol. Screen* **2012**, *17*, 421–434.
- (51) Yang, Y.; Kitagaki, J.; Dai, R. M.; Tsai, Y. C.; Lorick, K. L.; Ludwig, R. L.; Pierre, S. A.; Jensen, J. P.; Davydov, I. V.; Oberoi, P.; Li, C. C.; Kenten, J. H.; Beutler, J. A.; Vousden, K. H.; Weissman, A. M. Inhibitors of ubiquitin-activating enzyme (E1), a new class of potential cancer therapeutics. *Cancer Res.* **2007**, *67*, 9472–9481.
- (52) Zhao, B.; Choi, C. H. J.; Bhuripanyo, K.; Villhauer, E. B.; Zhang, K.; Schindelin, H.; Yin, J. Inhibiting the protein ubiquitination cascade by ubiquitin-mimicking short peptides. *Org. Lett.* **2012**, *14*, 5760–5763.
- (53) Schulman, B. A.; Harper, J. W. Ubiquitin-like protein activation by E1 enzymes: the apex for downstream signalling pathways. *Nat. Rev. Mol. Cell Biol.* **2009**, *10*, 319–331.
- (54) Huang, D. T.; Hunt, H. W.; Zhuang, M.; Ohi, M. D.; Holton, J. M.; Schulman, B. A. Basis for a ubiquitin-like protein thioester switch toggling E1-E2 affinity. *Nature* **2007**, *445*, 394–398.
- (55) Olsen, S. K.; Capili, A. D.; Lu, X.; Tan, D. S.; Lima, C. D. Active site remodelling accompanies thioester bond formation in the SUMO E1. *Nature* **2010**, *463*, 906–912.
- (56) Lois, L. M.; Lima, C. D. Structures of the SUMO E1 provide mechanistic insights into SUMO activation and E2 recruitment to E1. *EMBO J.* **2005**, *24*, 439–451.

☐ Recommended by ACS

Discovery of a PDZ Domain Inhibitor Targeting the Syndecan/Syntenin Protein-Protein Interaction: A Semi-Automated "Hit Identification-to-Optimization" Approach

Laurent Hoffer, Xavier Morelli, et al.

MARCH 20, 2023

JOURNAL OF MEDICINAL CHEMISTRY

READ 🗹

DNA-Encoded Macrocyclic Peptide Libraries Enable the Discovery of a Neutral MDM2-p53 Inhibitor

Anthony P. Silvestri, Joshua A. Schwochert, et al.

MAY 05, 2023

ACS MEDICINAL CHEMISTRY LETTERS

READ 🗹

Optimized M24B Aminopeptidase Inhibitors for CARD8 Inflammasome Activation

Qifeng Chen, Daniel A. Bachovchin, et al.

FEBRUARY 01, 2023

JOURNAL OF MEDICINAL CHEMISTRY

RFAD [✓

Design and Synthesis of Inhibitors of the E3 Ligase SMAD Specific E3 Ubiquitin Protein Ligase 1 as a Treatment for Lung Remodeling in Pulmonary Arterial Hypertension

Duncan E. Shaw, David Rowlands, et al.

JUNE 09, 2023

JOURNAL OF MEDICINAL CHEMISTRY

READ 🗹

Get More Suggestions >